Hydrogen Bonding, Solvent Exchange, and Coupled Proton and Electron Transfer in the Oxidation and Reduction of Redox-Active Tyrosine Y_Z in Mn-Depleted Core Complexes of Photosystem II†

Bruce A. Diner,‡* Dee Ann Force,§ David W. Randall,§,|| and R. David Britt§

Experimental Station, E. I. du Pont de Nemours & Co., Wilmington, Delaware 19880-0173, and Department of Chemistry, University of California, Davis, Davis, California 95616

Received August 6, 1998; Revised Manuscript Received October 27, 1998

ABSTRACT: The redox-active tyrosines, Y_Z and Y_D, of Photosystem II are oxidized by $P680^+$ to the neutral tyrosyl radical. This oxidation thus involves the transfer of the phenolic proton as well as an electron. It has recently been proposed that tyrosine Y_Z might replace the lost proton by abstraction of a hydrogen atom or a proton from a water molecule bound to the manganese cluster, thereby increasing the driving force for water oxidation. To compare and contrast with the intact system, we examine here, in a simplified Mn-depleted PSII core complex, isolated from a site-directed mutant of *Synechocystis* PCC 6803 lacking Y_D, the role of proton transfer in the oxidation and reduction of Y_Z. We show how the oxidation and reduction rates for Y_Z, the deuterium isotope effect on these rates, and the $Y_Z^\bullet - Y_Z$ difference spectra all depend on pH (from 5.5 to 9.5). This simplified system allows examination of electron-transfer processes over a broader range of pH than is possible with the intact system and with more tractable rates. The kinetic isotope effect for the oxidation of $P680^+$ by Y_Z is maximal at pH 7.0 (3.64). It decreases to lower pH as charge recombination, which shows no deuterium isotope, starts to become competitive with Y_Z oxidation. To higher pH, Y_Z becomes increasingly deprotonated to form the tyrosinate, the oxidation of which at pH 9.5 becomes extremely rapid (1260 ms^{-1}) and no longer limited by proton transfer. These observations point to a mechanism for the oxidation of Y_Z in which the tyrosinate is the species from which the electron occurs even at lower pH. The kinetics of oxidation of Y_Z show elements of rate limitation by both proton and electron transfer, with the former dominating at low pH and the latter at high pH. The proton-transfer limitation of Y_Z oxidation at low pH is best explained by a gated mechanism in which Y_Z and the acceptor of the phenolic proton need to form an electron/proton-transfer competent complex in competition with other hydrogen-bonding interactions that each have with neighboring residues. In contrast, the reduction of $Y_Z^\bullet$ appears not to be limited by proton transfer between pH 5.5 and 9.5. We also compare, in Mn-depleted *Synechocystis* PSII core complexes, Y_Z and Y_D with respect to solvent accessibility by detection of the deuterium isotope effect for Y_Z oxidation and by ^2H ESEEM measurement of hydrogen-bond exchange. Upon incubation of H_2O-prepared PSII core complexes in D_2O, the phenolic proton of Y_Z is exchanged for a deuterium in less than 2 min as opposed to a $t_{1/2}$ of about 9 h for Y_D. In addition, we show that $Y_D^\bullet$ is coordinated by two hydrogen bonds. $Y_Z^\bullet$ shows more disordered hydrogen bonding, reflecting inhomogeneity at the site. With ^2H ESEEM modulation comparable to that of $Y_D^\bullet$, $Y_Z^\bullet$ would appear to be coordinated by two hydrogen bonds in a significant fraction of the centers.

Photosystem II of oxygenic photosynthesis contains two redox-active tyrosines, Y_Z and Y_D,[1] each of which is oxidized by the photooxidized primary electron donor, $P680^+$, to form a phenoxyl radical (*1*). Y_Z is, by 4−6 orders of magnitude, the more rapid of the two to be oxidized and is the intermediate electron carrier between $P680^+$ and the Mn cluster, responsible for photosynthetic water oxidation. The function of Y_D is still unclear, though it may participate indirectly in the assembly or stabilization of the Mn cluster. Site-directed mutagenesis (*2*−*5*) and saturation recovery EPR (*6*) have localized Y_Z and Y_D, respectively, to residues Tyr161 of the D1 polypeptide and Tyr160 of the D2 polypeptide.

† Grants from the NRICGP/USDA (94-37306-0783) to B.A.D. and from the NSF (MCB 9513648) to R.D.B. are gratefully acknowledged. This paper is contribution No. 7817 of the Central Research and Development Department of E. I. du Pont de Nemours & Co.

‡ E. I. du Pont de Nemours & Co.

§ University of California, Davis.

|| Present address: Department of Chemistry, Stanford University, Stanford, California 94305.

[1] Abbreviations: CHES, 2-(*N*-Cyclohexylamino)ethane-sulfonic acid; Chl, chlorophyll; D1, one of two polypeptides of PSII responsible for the coordination of the primary and secondary electron-transfer components; D2, one of two polypeptides of PSII responsible for the coordination of the primary and secondary electron-transfer components; ENDOR, electron nuclear double resonance spectroscopy; ESEEM, electron spin−echo envelope modulation spectroscopy; FTIR, Fourier transform infrared spectroscopy; HEPES, *N*-(2-hydroxyethyl)piperazine-*N*′-(2-ethanesulfonic acid); MES, 2-(*N*-morpholino)ethanesulfonic acid; P680, primary electron donor chlorophyll(s) of PSII; pL, pH or pD; PSII, photosystem II; Q_A, primary plastoquinone electron acceptor; S2, two-equilvalent oxidized state of the Mn cluster; Y_D, a redox-active tyrosine located at position 160 of polypeptide D2; Y_Z, a redox-active tyrosine located at position 161 of polypeptide D1.

10.1021/bi981894r CCC: $15.00 © 1998 American Chemical Society
Published on Web 12/02/1998

Scheme 1. Rate Limitation by Proton or Electron Transfer[a]

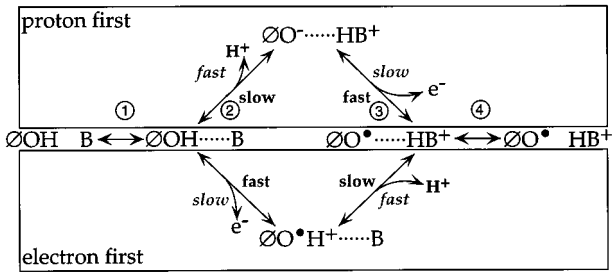

[a] Alternative pathways for tyrosine oxidation involving either proton transfer to the proton acceptor, B, (upper rectangle) or electron transfer to $P680^+$ (lower rectangle) as the primary event. In either pathway, either the electron transfer (relative rates marked in italics) or the proton transfer (relative rates marked in normal type) is rate-limiting. In the gated mechanism (see Discussion), reaction 1 would be rate-limiting.

The optical difference spectra for $Y_Z^\bullet - Y_Z$ (*7*−*9*) and $Y_D^\bullet - Y_D$ (*10*), the isotropic *g* values for $Y_Z^\bullet$ and $Y_D^\bullet$ (*1*, *11*), and their ENDOR (*12*−*17*), ESEEM (*18*, *19*) and FTIR spectra (*20*−*25*) all reinforce the conclusion that the oxidation of each of the two tyrosines results in the formation of the oxidized neutral radical from the neutral reduced form of the amino acid (for review, see ref *1*). The formation of the neutral tyrosyl radical, structural arguments based on magnetic coupling between $Y_Z^\bullet$ and the Mn cluster (*14*, *26*−*29*), and thermodynamic arguments (*30*−*35*), have together led to models proposing a direct role for Y_Z as a hydrogen atom (*36*−*37*) or proton abstractor (*14*) in the mechanism of water oxidation in Photosystem II. Such models involve the loss of a proton from Y_Z upon its oxidation (e.g., by delivery to the thylakoid lumen) followed upon reduction by reprotonation of Y_Z from a water bound to the manganese cluster. It has been argued (*34*−*35*) that coupling of the deprotonation of water to the oxidation of manganese increases the driving force of the oxidation. This interest in proton and electron transfer has led us to examine the mechanism by which these events are coupled in the oxidation and reduction of Y_Z. This work, for the most part on PSII core complexes depleted of Mn, will serve as a basis by which to compare and contrast the Mn depleted with the intact system.

The pathway for the oxidation and deprotonation of Y_Z can occur between either of two limiting cases (Scheme 1), one where the proton is lost first to a nearby base, followed by the electron, and the other where the electron is lost first, followed by the proton. This model is the tyrosine analogue of a model proposed earlier (*38*) for coupled electron and proton transfer in the quinone−iron complex of the purple bacterial reaction centers. In the first case, the tyrosine deprotonates to form the tyrosinate anion followed by the electron transfer. In the second case, tyrosine is oxidized to the cation radical followed by a proton transfer. For each of these pathways, either the proton or the electron transfer may be rate-limiting (see Scheme 1). It is also possible that the electron- and proton-transfer events are simultaneous as in a hydrogen atom transfer. To help distinguish between these cases, we study here, as a function of pH, the rates of oxidation and reduction of Y_Z, the kinetic deuterium isotope effect of both processes, and the ultraviolet spectrum of Y_Z. The results presented here provide support for the "proton first" pathway, with electron transfer occurring from the tyrosinate form of Y_Z.

The redox and kinetic behavior of Y_Z and Y_D are quite distinct (*1*), undoubtedly reflecting, respectively, different environmental influences and distances from the primary electron donor. While no crystal structure yet exists of Photosystem II, the environments of the two tyrosines have been constructed by homology modeling with the purple bacterial reaction centers (*39*−*41*) and probed by kinetic experiments using artificial reductants (*42*) and site-directed mutants (*43*−*49*, *70*). Y_Z has been proposed to be located in a substantially more polar environment than that of Y_D (*39*−*41*), one consistent with the likely nearby presence of the Mn cluster itself (*14*, *26*, *29*). One might expect that the greater polarity of the environment of Y_Z, its proximity to the Mn cluster, and the considerable distance measured for $Y_D^\bullet$ from the lumenal membrane surface (*50*−*51*), possibly due to extrinsic polypeptides that shield Y_D, would be reflected in differences in the accessibility of the two tyrosines to solvent. This accessibility is examined here by comparing the time course of proton/deuteron (H/D) exchange by two independent methods that monitor Y_Z and $Y_Z^\bullet$, respectively. We show H/D exchange to be far more rapid for Y_Z than for Y_D. Experiments probing the solvent accessibility of Y_Z have also been carried out in parallel by Tommos et al. (*52*).

This paper combines optical and magnetic resonance spectroscopies and kinetic methods to obtain new insights into coupled electron/proton transfer involving Y_Z, and proton/deuteron exchange and hydrogen bonding at both tyrosines.

EXPERIMENTAL PROCEDURES

Wild-type *Synechocystis* PCC 6803 used in these experiments is the glucose-tolerant strain described by Williams (*53*). The Y_D-less strain (D2−Tyr160Phe) is that described in Tang et al. (*15*). Oxygen-evolving PSII-enriched "BBY" membranes were isolated from market spinach using a modification of the method of Berthold et al. (*54*−*56*). The membranes were prepared and exchanged with D_2O and/or treated with acetate as described by Force et al. (*57*) (see also refs *35*, *58*).

Manganese-depleted Photosystem II core complexes from *Synechocystis* 6803 wild type and Y_D-less mutant were prepared as described in Tang et al. (*15*), desalted, and suspended in 50 mM MES−NaOH, pH 6.0, containing 20 mM $CaCl_2$, 5 mM $MgCl_2$, 25% (w/v) glycerol, and 0.03% dodecyl maltoside. Final concentrations were typically 5−10 mg of Chl/mL and were stored at −80 °C.

Optical measurements were performed in a home-built instrument similar to that originally described by Joliot et al. (*59*) using a Jobin-Yvon HL300 monochromator. Detecting flashes were provided by EG&G FX199 (glass) and FX199U (quartz) flash lamps, and saturating actinic flashes were provided by a linear flash lamp pulsed dye laser (Model LFDL-3, Cynosure Inc.). The kinetic curves in all cases were fit by the sum of two exponentials. For the reduction of $P680^+$, the major component typically contributed ≥75% of the total relaxation. While the time resolution of this instrument is 1 μs, the 0 time points for the fast relaxations of $P680^+$ at alkaline pH could be determined by dropping the pH to 6.5 for the same sample and measuring the signal

amplitude during the lifetime of the actinic flash. Measurements of the reduction of Q_A with a much longer lifetime were used to verify that the saturating flash yield of charge separation was not influenced by the pH. The relaxation of $P680^+ - P680$ was measured at 432.5 nm, the wavelength of maximal bleaching in the Soret, and that of $Q_A^- - Q_A$ at the wavelength maximum at 325 nm.

The preparation of samples for optical kinetic isotope effect experiments involved diluting *Synechocystis* PSII core complexes into H_2O or D_2O buffers to a final concentration of 10−14 μg of Chl/mL in 10 mM NaCl plus 20 mM MES−NaOH(D) for pL (pH or pD) 5.5−6.5, 20 mM HEPES−NaOH(D) for pL 7.5−8.5, and 20 mM CHES−NaOH(D) for 9.0−9.5. The samples also contained 2 μM $K_3Fe(CN)_6$ and 10 μM EDTA. The pD was measured in D_2O buffers by adding 0.4 to the reading on the pH meter.

The time course for H/D exchange was also examined using ESEEM. PSII core complexes were diluted 1:2 into 20 mM HEPES−NaOD, pD 7.5, and 10 mM NaCl in D_2O giving a final concentration of 66% D_2O. The final pL was $\sim$ 7.0. $K_3Fe(CN)_6$ (300 μM) was also added at time 0. The samples were incubated on ice for various lengths of time up to 25 h at which point $Y_Z^\bullet$ and $Y_D^\bullet$ were generated and trapped as described below.

$Y_D^\bullet$ was trapped by illuminating for 30 s in an EPR tube at 0 °C (transparent dewar with ice water) wild-type PSII core complexes in the presence of 300 μM $K_3Fe(CN)_6$. White light at an intensity of 500 W/m^2 was provided by a 150 W tungsten−halogen lamp (Cuda Products Inc., Model I-150). The core complexes were then incubated on ice in the dark. After 15 min the sample was frozen in the dark in liquid nitrogen and stored in a liquid nitrogen dewar until measured.

$Y_Z^\bullet$ was trapped in an EPR tube using a transparent dewar containing liquid N_2 by freezing under white illumination at 5000 W/m^2 (total duration $\leq$20 s) PSII core complexes in the presence of 300 μM $K_3Fe(CN)_6$ (*15*). The PSII core complexes were from the Y_D-less strain of *Synechocystis* 6803. The samples were stored in liquid nitrogen until measured.

Continuous optical spectra were obtained on a model 2101-PC (Shimadzu) UV−vis recording spectrophotometer.

ESEEM (Electron Spin−Echo Envelope Modulation) experiments were performed with a laboratory-built pulsed EPR spectrometer (*60*). Two-pulse time domain ESEEM experiments were performed by incrementing the time τ in the echo sequence: $\pi/2$-τ-π-echo, while three-pulse time domain ESEEM experiments were performed by incrementing the time T in the stimulated echo sequence: $\pi/2$-τ-$\pi/2$-T-$\pi/2$-τ-stimulated echo, choosing a fixed τ value to maximize the contribution of the deuteron frequency component while suppressing that due to protons (*61*, *62*).

Frequency domain spectra were obtained from the time domain modulation patterns following reconstruction of the instrumental dead time using a cosine Fourier backfill method (*63*). Spectral normalization of D_2O/H_2O sample pairs with subsequent D/H ratioing was as described by Force et al. (*57*). Computer simulations of the time domain data were performed as previously described (*64*) on the basis of the density matrix formalism developed by Mims (*65*).

RESULTS

Kinetic Deuterium Isotope Effects. Y_Z Oxidation and $P680^+$ Reduction. We have attempted to characterize the oxidation pathway for Y_Z by measuring the effect of H/D exchange on the kinetics of oxidation of Y_Z by $P680^+$. This was accomplished by incubating non-oxygen-evolving Y_D-less PSII core complexes in the presence of H_2O or D_2O (>99%) as described in the Experimental Procedures and measuring $P680^+$ reduction (Y_Z oxidation) at 432.5 nm. This wavelength corresponds to the maximum bleaching observed for $P680^+ - P680$ in PSII core complexes from *Synechocystis* (*5*).

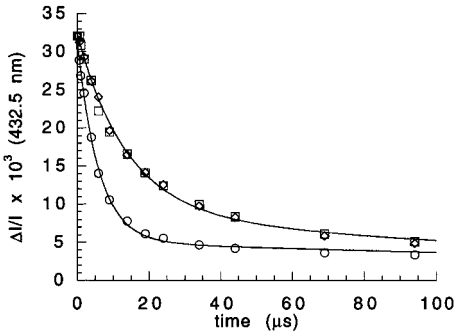

FIGURE 1: Kinetics of oxidation of Y_Z as measured by the reduction of $P680^+$ at 432.5 nm following a saturating actinic laser flash at pL 7.5. PSII core complexes were diluted to 14 μg of Chl/mL in H_2O buffer (○) or D_2O buffer (□, ◇). In D_2O the sample was either tested immediately (within 2 min of dilution, ◇) or incubated for 3.5 h on ice □). In the case of immediate testing in D_2O buffer, the first time point was measured at 20 μs after the actinic flash after which the other points were measured on the same sample with 1 min of dark incubation between each measurement.

An example of such an experiment is shown in Figure 1 where, at pL 7.5, replacement of H_2O with D_2O slows the rate of oxidation of Y_Z by approximately a factor of 2.5. This observation, however, does not distinguish whether the kinetic deuterium isotope effect arises from proton (deuteron) transfer associated with the oxidation of Y_Z or with the reduction of $P680^+$. In an attempt to distinguish between the two, we looked for a deuterium isotope effect on the reduction of $P680^+$ by Q_A^- (charge recombination), in a mutant lacking Y_Z (mutant D1−Tyr161Phe (*5*)). The wild-type and mutant PSII core complexes isolated here lack Q_B, so that on the acceptor side of the reaction center the electron can go no further than Q_A. Therefore, in the Y_Z-less mutant, the charged pair $P680^+Q_A^-$ is formed and it is this species that undergoes charge recombination without further equilibration with secondary electron acceptors or donors. Y_D does not interfere as it reacts too slowly ($k = 60$ s^{-1} (*66*)) compared to the rate of charge recombination ($k = 700$ s^{-1} (*5*)). This reaction was monitored at both 325 nm (λ_{max} for $Q_A^- - Q_A$) and at 432.5 nm (λ_{min} for $P680^+ - P680$). Measurements at pL 7.5 (Figure 2, 432.5 nm) show a negligible difference between the rate of charge recombination in the presence of H_2O and D_2O. While this reaction is substantially slower than the rate of reduction of $P680^+$ by Y_Z, time points in the microsecond time range (325 nm, not shown) show no hint of a deuterium isotope effect. We therefore attribute to the tyrosine alone the observed deuterium isotope effect upon oxidation of Y_Z. Further support for this conclusion is provided below.

Rate of H/D Exchange Measured by the Kinetic Isotope Effect. The samples used for the kinetic deuterium isotope effect experiments were initially incubated overnight to ensure complete exchange of H_2O with D_2O. This long incubation was found to be unnecessary as shown in Figure

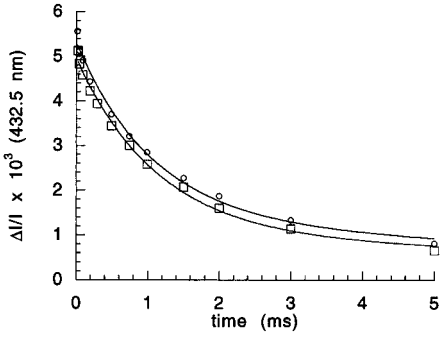

FIGURE 2: Kinetics of charge recombination between $P680^+$ and Q_A^- measured in H_2O (○) and D_2O (□) buffer following a saturating actinic laser flash at 432.5 nm. PSII core complexes from the Y_D-less mutant D1-Tyr161Phe were suspended in the same buffer as that in Figure 1.

1. Here a sample prepared in H_2O was incubated for either 3 h 30 min at 4 °C or the minimum time it took to prepare the sample (~2 min at room temperature). The first time point measured was that at 20 μs following the saturating actinic flash, a time point that shows a large contrast between H_2O and D_2O equilibrated samples. The 2 min sample gave the same amplitude at this time point as that shown by the sample incubated for the much longer period. The complete experiment, which took an additional 30 min to perform, showed no difference between the two incubations and between these and an overnight incubation (not shown), indicating that the exchange implicated in the deuterium isotope effect had gone to completion within two minutes. Ahlbrink et al. (*77*) have made a similar observation in Mn-depleted PSII core complexes.

Rate of H/D Exchange Measured by Deuterium Bonding to $Y_Z^\bullet$. To help localize the origin of the kinetic deuterium isotope effect to the immediate environment of Y_Z, we used ESEEM to show by another method, this one sensitive to the radical $Y_Z^\bullet$, that such exchange actually does occur on a time scale consistent with the appearance of the deuterium isotope effect measured optically.

It was previously shown that the phenolic oxygen of both tyrosines, $Y_Z^\bullet$ (*13*, *15*, *67*) and $Y_D^\bullet$ (*18*, *20*−*21*, *67*−*68*), is hydrogen-bonded. The ESEEM technique can be used to specifically detect the replacement with deuterons of the hydrogen-bonded protons to the phenolic oxygen of the tyrosyl radical. It was shown, in the case of Y_D, that this tyrosine hydrogen bonds to D2−His189 in its reduced form (*21*) and is hydrogen bonded by this same histidine in its oxidized form (*21*, *45*, *47*, *69*). Thus, it is likely that the same proton is involved in both hydrogen bonds as it rocks back and forth (*36*) between Y_D and D2−His189. The same is likely true of Y_Z and its proton acceptor. The ESEEM measurement should, therefore, also indicate the rate at which H/D exchange has occurred on the phenolic hydroxyl group of Y_Z. The identity of the proton acceptor associated with Y_Z is for the moment unclear. While kinetic evidence would point to D1−His190 as the proton acceptor (*25*, *43*, *49*, *70*), $Y_Z^\bullet$ ENDOR does not support this assignment (see below, Campbell, Britt, and Diner, manuscript in preparation).

PSII core complexes of *Synechocystis* wild-type and Y_D-less mutant D2−Tyr160Phe were isolated and concentrated in H_2O. They were then diluted 3-fold in D_2O buffer (final concentration 66% D_2O) at time 0 (pL = 7.0), placed in EPR tubes, and incubated for increasing times at 0 °C in the dark. $Y_Z^\bullet$ and $Y_D^\bullet$ were trapped as described in Experimental Procedures and the samples stored in liquid N_2. The two-pulse ESEEM spectra (Figure 3) of the radicals were recorded on samples trapped at the indicated times. The amplitude of the signal arising from the deuterium hyperfine coupling to the electronic spin of the radical is a measure of the replacement of protons with deuterons in the immediate vicinity of the radical (to within a distance of ~3 Å, including those involved in hydrogen bonding (vide infra). This experiment shows that H/D exchange of protons in immediate proximity to $Y_Z^\bullet$ occurs as fast as the sample can be prepared (<10 min), consistent with the rapid appearance of the deuterium isotope effect for the oxidation of Y_Z. As the proton hydrogen-bonded to the radical likely originates from the phenolic hydroxyl of the reduced tyrosine, this experiment would argue that the H/D exchange on the phenolic hydroxyl occurs on the same time scale. This view is consistent then with the deuterium isotope effect appearing as a consequence of exchange at the OH (OD) bond of Y_Z. Even if the deuterium isotope effect did not originate from exchange at the phenolic hydroxyl, both rates of exchange experiments indicate rapid communication between Y_Z and the bulk solvent. While the half time for H/D exchange for $Y_Z^\bullet$ is much less than the time it takes to prepare the sample (10 min for ESEEM, 2 min for the optical experiment), that for $Y_D^\bullet$ is much longer, on the order of 9 h (Figure 3). This observation is consistent with earlier observations that showed that H/D exchange of the proton hydrogen bonded to $Y_D^\bullet$ is quite slow, requiring overnight incubation (*47*, *68*). While there is some fast phase associated with H/D exchange at $Y_D^\bullet$ (Figure 3), these experiments indicate that Y_Z is in far more rapid communication with the solvent water than is Y_D, consistent with the closer proximity of Y_Z to the water-oxidizing manganese cluster, its greater accessibility to reductants (*42*), its more polar environment (*39*−*41*), and the deeply buried environment ascribed to Y_D (*50*, *51*).

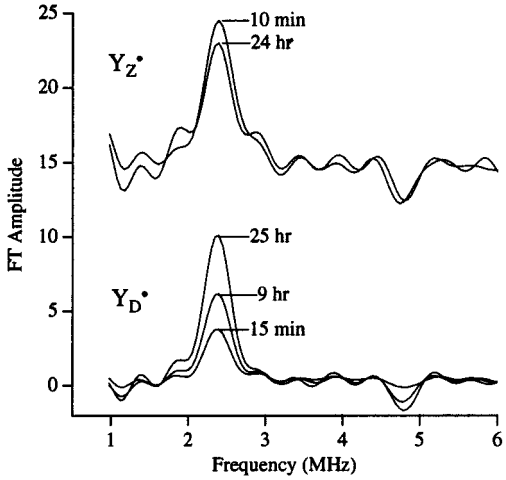

FIGURE 3: Frequency domain for D/H ratioed two-pulse ESEEM spectra of $Y_Z^\bullet$ in Mn-depleted PSII core complexes from *Synechocystis* mutant D1−Tyr161Phe and $Y_D^\bullet$ in Mn-depleted Synechocystis wild-type PSII core complexes. The PSII cores were diluted 3-fold into D_2O buffer (final concentration 66% D_2O) and incubated on ice for the times indicated. For additional details see Experimental Procedures. Instrument parameters: ν_{MW} = 10.199 GHz; MW power ≈ 50 W; B = 3643 G; starting τ = 120 ns; $\pi/2$ = 15 ns; repetition rate = 25 Hz; temperature = 10.0 K.

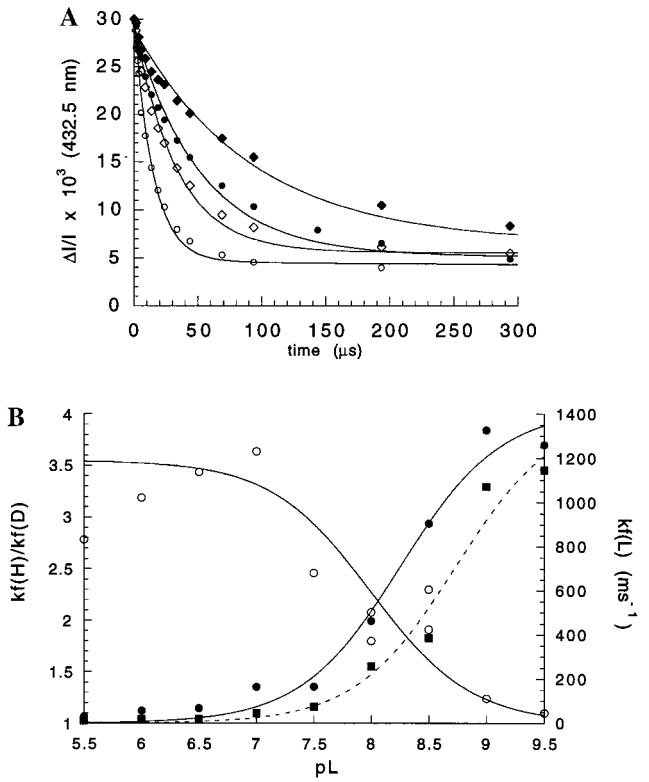

FIGURE 4: (A) Kinetics of oxidation of Y_Z, measured as the reduction of $P680^+$ at 432.5 nm following a saturating actinic laser flash at pL 5.5 (◇, ◆) and 6.5 (○, ●). PSII core complexes were diluted (see Experimental Procedures) to 13 μg of Chl/mL in H_2O buffer (open symbols) or D_2O buffer (closed symbols). (B) Dependence on pL of the rates of oxidation (k_f) of Y_Z by $P680^+$ in H_2O (●, solid line) and D_2O (■, dashed line) and of the kinetic deuterium isotope effect ($k_f(H)/k_f(D)$, ○, solid line). The k_f points for H_2O and D_2O are fit by a theoretical curve for the dissociation of the weak acid tyrosine to form tyrosinate with pK_a values of 8.3 and 8.7, respectively. The plotted rate constant, k_f, corresponds to the faster and major component (≥75%) of the biexponential curve fits at each pL. The theoretical curve for the deuterium isotope effect ($k_f(H)/k_f(D)$) is the ratio of the tyrosinate concentration in H_2O to that in D_2O with pK_a values of 8.0 and 8.55, respectively.

Table 1. Rate Constants and Deuterium Isotope Effects for the Oxidation of Y_Z

pL	$k_f(H)$ (ms^{-1})	$k_f(D)$ (ms^{-1})	$k_f(H)/k_f(D)$
5.5	30.6	11	2.78
6.0	55.9	17.5	3.19
6.5	67.0	19.5	3.44
7.0	164	45	3.64
7.5	170	69	2.46
8.0	463	257	1.80
8.5	905	387	2.30
9.0	1326	1071	1.24
9.5	1260	1146	1.10

Dependence of Kinetic Isotope Effect on pL. The kinetic deuterium isotope effect for the rate of oxidation of Y_Z by $P680^+$ (k_f) shows a marked dependence on pL. Experiments at pL 5.5 and 6.5 (Figure 4A) show an even larger kinetic isotope effect than at pL 7.5 (Figure 1). The effect is maximal at pL 7.0 (3.64, Table 1), decreasing to lower pL, and decreasing to higher pL until it virtually disappears at pL 9.5 where $k_f(H)/k_f(D)$ is equal to 1.1. The dependence on pL of the rate of electron transfer and of the isotope effect is shown in Figure 4B (Table 1). These appear to be correlated, with pK_as of 8.3 and 8.0, respectively. One possible explanation for this pL dependence is that, as the pL rises, there is a shifting of the hydrogen-bonding phenolic proton from the phenolic oxygen to the proton acceptor, thereby increasing the tyrosinate character of the reduced tyrosine. Were the rate of Y_Z oxidation limited by the rate of formation or concentration of tyrosinate and were these diminished by the replacement of H_2O with D_2O, then, as observed, the effect of H/D exchange on the rate of oxidation of Y_Z would diminish and the rate of electron transfer would increase with pL.

To explore the possibility of an increasing proton dissociation with increasing pL, we examined (Figure 5A) the oxidized-minus-reduced difference spectrum, $Y_Z^\bullet - Y_Z$, at pH 6.1 and 9, close to the limits over which the kinetic isotope effect was examined (Figure 4B, Table 1). The spectra were measured at −6 °C, using the conditions described in Diner et al. (*10*). Compared to room temperature, these conditions slow the reduction of $Y_Z^\bullet$ more than they slow the oxidation of Q_A^-, allowing the $Y_Z^\bullet - Y_Z$ difference spectrum to be measured with reduced interference from $Q_A^- - Q_A$. An alteration in the UV difference spectrum is observed upon raising the pH. The UV absorbance spectrum of tyrosine in water was measured at pH 7.4 and 12, below and above, respectively, the pK_a = 10.9 for the tyrosine phenolate/phenol couple in solution. Figure 5B shows the marked effect that the dissociation of the phenolate proton has on the absorption spectrum of tyrosine. The double difference spectrum $(Y_Z^\bullet - Y_Z)_{pH\,9} - (Y_Z^\bullet - Y_Z)_{pH\,6.1}$ was compared (Figure 5C) with the difference spectrum of tyrosine in water $\Delta A_{pH7.4-pH12}$. Assuming the spectrum of the radical to be insensitive to pH, the double difference spectrum should give the difference in the reduced tyrosine spectrum in situ at the lower minus the higher pH. The solution and the biological difference spectra show considerable similarity despite their vertical displacement and their different rates of decline below 260 nm. Assuming as well that the extinction coefficients for tyrosine and tyrosinate are the same in solution as in the protein, then a comparison of the amplitude ($\Delta A_{273-293\ nm}$) of the double difference spectrum for Y_Z with that of the model spectrum ($\epsilon_{273-293\ nm}$ = 2350 M^{-1} cm^{-1}) should give the Y_Z tyrosinate concentration at pH 9.0. This comparison indicates that, at this pH, a little over half of the Y_Z (~60%) is in the tyrosinate form. This observation is somewhat less than that predicted for a pK_a of between 8.0 and 8.3 observed for the pL dependence of $k_f(H)/k_f(D)$ and of $k_f(H)$, respectively. Reasons for the underestimate of the tyrosinate concentration and for the differences between the biological and solution spectra may stem from small errors arising from the two assumptions: (1) that the extinction coefficients are the same in the reaction center and in water; and (2) that the spectrum of $Y_Z^\bullet$ is the same at the two pHs.

All of the above observations indicate that the in situ pK_a for Y_Z is shifted to lower pH compared to tyrosine in solution, probably through the association of Y_Z with a proton acceptor (e.g., D1−His190). That the rate of electron transfer increases and the deuterium isotope effect falls off with increasing pL over the same range at which the Y_Z deprotonates to form the tyrosinate Y_Z^-, would therefore be consistent with a model that follows the upper pathway of Scheme 1 and where the tyrosinate is the active form of Y_Z for electron transfer.

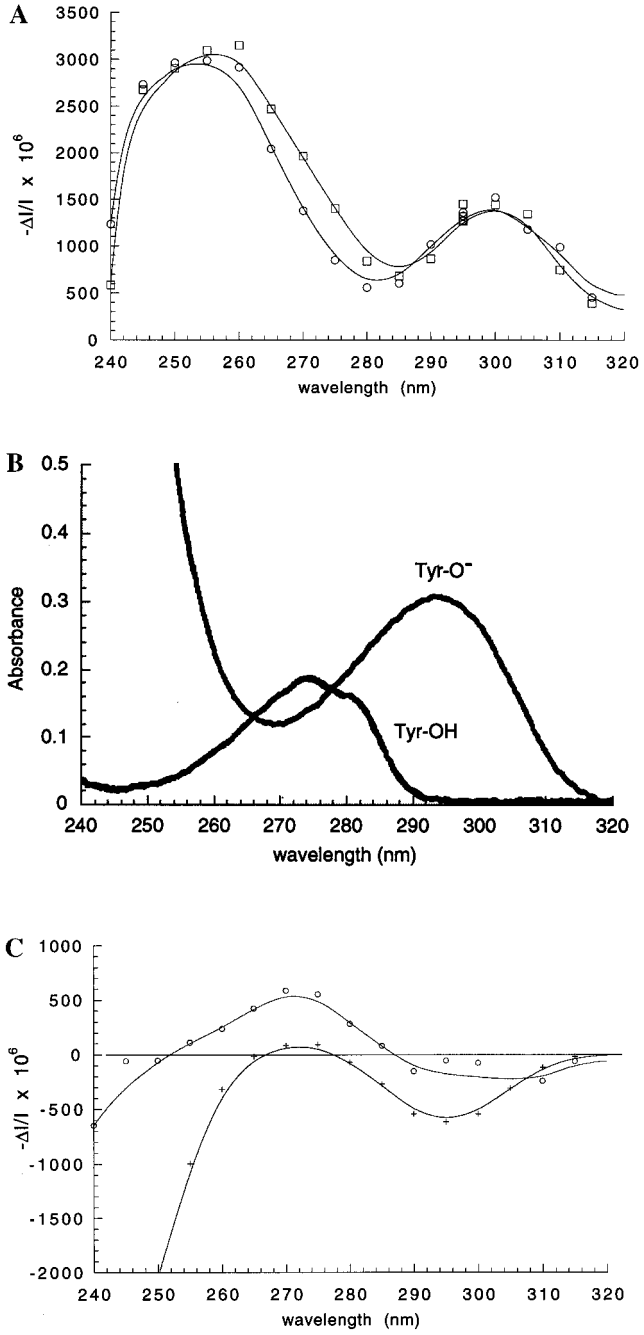

FIGURE 5: (A) Difference spectrum ($Y_Z^\bullet - Y_Z$) measured at pH 6.1 (○) and pH 9.0 (□) in the UV. PSII core complexes were suspended at 10 μg of Chl/mL in either 40 mM MES, pH 6.1 or 50 mM CHES, pH 9.01, plus 25% glycerol, 5 mM $MgCl_2$, 20 mM $CaCl_2$, 0.03% dodecyl maltoside, and 600 μM $K_3Fe(CN)_6$. The samples were cooled to −6 °C by flowing a stream of cold nitrogen around the spectrophotometer cuvette. Absorbance changes were monitored at 600 ms following a single saturating flash, a time long compared to the lifetime of Q_A^- ($t_{1/2}$ ~50 ms). Both spectra have been corrected for the difference ferro-ferricyanide and for residual $Q_A^- - Q_A$. (B) Absorption spectra of tyrosine (150 μM) at pH 7.4 (Tyr-OH) and pH 12.0 (Tyr-O^-) in water. (C) Double difference spectrum ($\Delta\Delta I/I$) of $Y_Z^\bullet - Y_Z$ at pH 9 minus $Y_Z^\bullet - Y_Z$ at pH 6.1 (○) from part A compared to the tyrosine-minus-tyrosinate difference spectrum at pH 7.4 minus that at pH 12 (+). The latter spectrum has been scaled to the same difference at 273 nm minus 293 nm for the $\Delta\Delta I/I$ of Y_Z. The amplitude of the model spectrum at 273 nm minus 293 nm corresponds to about 60% of the amplitude expected were all the centers in the tyrosinate form at pH 9 and assuming that the tyrosinate/tyrosine extinction coefficients are the same in water and in reaction centers and that the spectra of $Y_Z^\bullet$ are the same at both pHs.

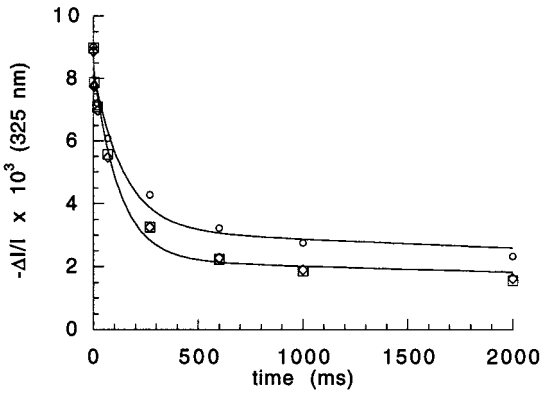

FIGURE 6: Kinetics of charge recombination measured at 325 nm between $Y_Z^\bullet$ and Q_A^- following a saturating actinic laser flash. The same samples were used as in Figure 1: H_2O buffer (○), D_2O buffer (◇, □) measured immediately (◇) and after 3.5 h (□).

Reduction of $Y_Z^\bullet$. In evaluating the role of protons in the oxidation of the Mn cluster by $Y_Z^\bullet$, it is important to know what contribution to the kinetic isotope effect comes from $Y_Z^\bullet$ reduction itself. The Mn-depleted case is relevant to the one where the Mn cluster is intact as the FTIR difference spectrum for $Y_Z^\bullet/Y_Z$ shows very little difference in the presence or absence of the Mn cluster (*25*).

The role of protons in the reduction of $Y_Z^\bullet$ can be determined by measurement of the rate of charge recombination between Q_A^- and the donor side (k_{obs}). Such charge recombination occurs through the $P680^+Q_A^-$ couple, the rate of reaction of which (k_{in}, 700 s^{-1} (*5*)) has been shown to be pH-independent (*71*−*72*). The rate of charge recombination between $P680^+$ and Q_A^- was also examined above and shown to have no isotope effect. Where equilibration between Y_Z and P680 is rapid with respect to the rate of recombination (k_f, $k_b \gg k_{in}$), the rate of charge recombination depends on the equilibrium constant, K_{zp}, for the reaction $Y_ZP680^+ \leftrightarrow Y_Z^+P680$. Here Y_Z^+ designates the tyrosyl radical−proton acceptor complex. Having determined the deuterium isotope effect for k_f, one can calculate the deuterium isotope effect for k_b from the effect of H/D exchange on K_{zp}.

$$Y_ZP^+ \underset{k_b}{\overset{k_f}{\rightleftharpoons}} Y_Z^+P \quad (1)$$

$$K_{zp} = [Y_Z^+P]/[Y_ZP^+] = k_f/k_b \quad (2)$$

$$k_{obs} = k_{in}/(K_{zp} + 1) \quad (3)$$

$$k_b(H)/k_b(D) = [k_f(H)/k_f(D)][K_{zp}(D)/K_{zp}(H)] \quad (4)$$

The rate of charge recombination between Q_A^- and $Y_Z^\bullet$ was measured at 325 nm ($Q_A^- - Q_A$) as a function of pL and in H_2O or D_2O in Y_D-less PSII core complexes. An example is shown in Figure 6 of recombination measured at pL 7.5 in Y_D-less PSII core complexes. The kinetic deuterium isotope effect for the recombination (k_{obs}) was examined over the same range of pL (5.5−9.5) as above for oxidation of Y_Z. The results (Table 2) show that there is a weaker isotope effect (approximately 2) for the reduction of $Y_Z^\bullet$ (k_b) than for the oxidation. Both the rate of reduction, k_b, and the kinetic isotope effect for reduction, $k_b(H)/k_b(D)$, show very little dependence on pL over the range examined, reflecting more likely a solvent reorganization than a rate limited by a

Table 2. Rate Constants and Deuterium Isotope Effects for the Reduction of Y_Z

pL	k_{obs}(H) (ms^{-1})	k_{obs}(D) (ms^{-1})	k_{obs}(H)/k_{obs}(D)	k_b(H) (ms^{-1})	k_b(D) (ms^{-1})	K_{zp}(H)	K_{zp}(D)	k_b(H)/k_b(D)
5.5	0.0370	0.0650	0.554	1.66	1.12	18.4	9.8	1.48
6.0	0.0253	0.0439	0.576	2.02	1.10	27.7	15.9	1.83
6.5	0.0173	0.0273	0.669	1.70	0.79	39.5	24.6	2.14
7.5	0.0066	0.0081	0.815	1.58	0.88	105	85.4	1.80
8.5	0.00376	0.00312	1.205	2.04	0.89	185	223.4	2.29
9.0	0.00194	0.00126	1.540	3.68	1.93	360	554	1.90
9.5	0.00209	0.00165	1.267	3.35	2.40	334	423	1.40

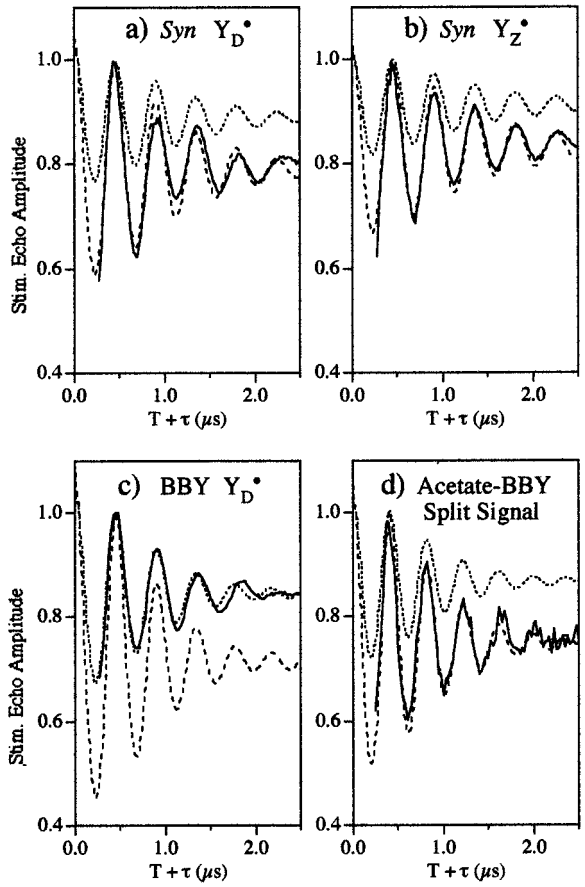

FIGURE 7: Time domain for $^2H/^1H$ ratioed 3-pulse ESEEM spectra of (a) $Y_D^•$ in Mn-depleted wild-type *Synechocystis* PSII core complexes (pL = 7.0, exchange time = 24 h at 4 °C), (b) $Y_Z^•$ in Mn-depleted PSII core complexes from the *Synechocystis* Y_D-less mutant (D2−Tyr160Phe) (pL = 6.1, exchange time = 24 h at 4 °C), (c) $Y_D^•$ in spinach BBY particles (pL = 6.0, exchange time = 24 h at 4 °C) and (d) the split signal of acetate-treated spinach BBYs (pL = 5.5, exchange time = 1.5 h at 4 °C). All of these samples are in 100% D_2O buffer with the exception of the *Synechocystis* $Y_D^•$ sample which is in 66% D_2O and has been scaled to 100%. The experimental data are shown as solid lines; the simulations are short dashes for one ^2H and long dashes for two ^2H. Instrument parameters: ν_{MW} = 9.430 GHz (a and b), 9.203 GHz (c), 10.013 GHz (d); MW power ≈ 50 W; B = 3368 G (a and b), 3292 G (c), 3650 G (d); τ = 209 ns (a and b), 214 ns (c), 210 ns (d); $\pi/2$ = 15 ns; repetition rate = 25 Hz (a−c), 200 Hz (d); temperature = 4.2 K. Simulation parameters: A_{iso} = −50 kHz (a and b), 0 kHz (c and d); e^2Qq = 170 kHz (a and b), 200 kHz (c and d); η = 0; T_{dip} = 470 kHz (a), 407 kHz (b), 570 kHz (c and d).

proton transfer. These observations are consistent with a reduction of the neutral $Y_Z^•$ to the tyrosinate, Y_Z^-.

Numbers of Hydrogen Bonds to $Y_Z^•$ and $Y_D^•$. We have previously used ^2H pulsed ENDOR to accurately determine hyperfine and quadrupolar couplings to deuterons exchanged into the hydrogen bond of $Y_D^•$ and $Y_Z^•$ (*13*). Using ENDOR-derived coupling parameters, we can then simulate the time domain ESE modulation patterns, varying only the number of deuterons in the simulation in order to quantify the number of deuterons with that class of couplings (*57*) introduced after a given time of incubation in D_2O-enriched buffer. Figure 7 shows the results of such constrained simulations for *Synechocystis* $Y_D^•$ (Figure 7a, pL = 7.0, exchange time = 24 h at 4 °C), *Synechocystis* $Y_Z^•$ (Figure 7b, pL = 6.1, exchange time = 24 h at 4 °C), Mn cluster intact spinach "BBY" membrane $Y_D^•$ (Figure 7c, pL = 6.0, exchange time = 24 h at 4 °C), and Mn cluster intact but inhibited by acetate treatment of spinach "BBY" membrane S2−$Y_Z^•$ split signal (Figure 7d, pL = 5.5, exchange time = 1.5 h at 4 °C). The Fourier transforms of these time domain ESEEM patterns are shown in Figure 8, where it is immediately apparent that the *Synechocystis* $Y_Z^•$ and $Y_D^•$ and the spinach S2−$Y_Z^•$ split signal all exhibit much greater modulation than the spinach $Y_D^•$.

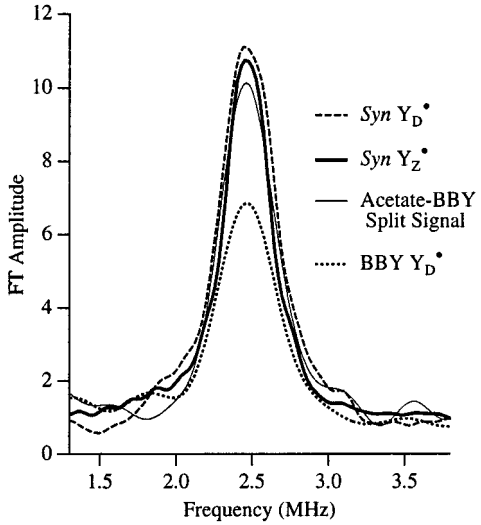

FIGURE 8: Frequency domain three-pulse ESEEM spectra obtained by Fourier transform of the experimental time domain modulation from Figure 7.

The constrained time domain simulations provide a quantitative measure of the numbers of deuterons for each case. For example, for $Y_D^•$ in spinach "BBY" membranes, using the 570 kHz dipolar coupling determined from ENDOR, the time domain ESEEM pattern is fit reasonably well using a single deuteron (Figure 7c) (*57*). The ^2H ENDOR pattern of the S2−$Y_Z^•$ split signal is less resolved than that of $Y_D^•$, but shows a similar overall splitting pattern. The ESEEM fits well using two deuterons with the same 570 kHz dipolar coupling used for the $Y_D^•$ simulation (Figure 7d). We had originally considered this to be very strong evidence that $Y_Z^•$ participates in two hydrogen-bonding interactions in the S2−$Y_Z^•$ state of acetate-treated spinach

membranes (*57*). However our recent observation (*29*) of ^{55}Mn ENDOR in this S2−$Y_Z^•$ state shows that there is significant "Mn character" in this coupled signal, raising the possibility that deuteron modulation in this and other split signal forms (*52*) may arise from deuterons exchanged into the Mn site as well as the tyrosine site. This point has also recently been made by Dorlet et al. (*73*) on the basis of split signal EPR simulations. Therefore, the exact nature of $Y_Z^•$ hydrogen bonding in the S2−$Y_Z^•$ state currently remains an open question.

The ^{2}H ENDOR of $Y_D^•$ in Mn-depleted *Synechocystis* particles was simulated with a slightly smaller dipolar coupling (470 kHz) along with a small isotropic component (−50 kHz) (*13*). By using these parameters, we obtain a better simulation of the ESEEM using two deuterons rather than one (Figure 7a). We therefore favor a picture whereby $Y_D^•$ in Mn-depleted *Synechocystis* forms two approximately equivalent strength hydrogen bonds that undergo ^{2}H exchange under the experimental conditions used here. This contrasts with the Mn intact spinach case where only one ^{2}H exchanges into a hydrogen-bonding site in 24 h. What is not currently clear is whether this difference reflects a true difference in the number of hydrogen bonds for $Y_D^•$ in spinach versus *Synechocystis*. Alternatively, the number may depend on the state or presence of the Mn cluster, or other intrinsic differences between Mn-depleted *Synechocystis* particles, including their lack of the 17 and 23 kDa extrinsic polypeptides, when compared to intact "BBY" spinach membranes. These may affect the exchange rate of ^{2}H into the deeply buried Y_D site.

In contrast to the ESE-ENDOR spectrum that shows well-defined hydrogen bonding to $Y_D^•$, the ESE-ENDOR spectrum of $Y_Z^•$ trapped in Mn-depleted *Synechocystis* particles shows a broad structureless feature (*13*). The breadth is, however, approximately equivalent to that of the hydrogen-bonded $Y_D^•$ radical, but a factor of 3 greater than what we observe for the H-bondless tyrosine radical in *Escherichia coli* ribonucleotide reductase (*57*). These observations led us to argue for strong but disordered hydrogen bonding for $Y_Z^•$ in Mn-depleted *Synechocystis* particles (*13*), a description also supported by cw ENDOR (*15*) and high field EPR (*74*). In this work, we observe (Figure 8) that the ESEEM modulation depth for $Y_Z^•$ is approximately equal to that of the *Synechocystis* $Y_D^•$, which we attribute to two hydrogen bonds, and a good fit to the ESEEM is obtained with two equivalently coupled deuterons (Figure 7b, 407 kHz dipolar coupling). However, from the ENDOR there is no basis for carrying out such simulations using only a single well-defined class. For example, utilizing two dissimilarly coupled deuterons (553 and 283 kHz) also gives a good fit to the ESEEM data (not shown). In reality, there is likely a distribution of couplings from multiple deuterons rapidly exchanged into the $Y_Z^•$ site in the Mn-depleted *Synechocystis* particles. Similar results were reported for Mn-depleted spinach PSII membranes (*52*) with a favored simulation resulting from one strongly interacting deuteron and several more weakly coupled deuterons.

DISCUSSION

Oxidation of each of the two redox-active tyrosines of Photosystem II over most of the physiological pH range results in the formation of a neutral radical from the neutral phenol. Under these conditions, proton transfer must, therefore, accompany electron transfer.

There are several observations that favor the upper pathway of Scheme 1 (tyrosinate intermediate) as the mechanism by which proton and electron transfer are coordinated in Y_Z oxidation. We observe an increase in the rate of electron transfer (*75*,*76*) and a decrease in the kinetic deuterium isotope effect with increasing pL over the same range (from 7.0 to 9.5, Figure 4B) and with similar pK_as (8.3 and 8.0, respectively). Over this same pH range there is an evolution of the difference spectrum, ($Y_Z^•$ − Y_Z), that resembles an increased deprotonation of tyrosine toward the tyrosinate as the pH increases. This deprotonation is also supported by preliminary FTIR data that shows at 1238 cm^{-1} the disappearance of a δC−O−H bending mode for Y_Z between pH 8 and 9 (Catherine Berthomieu, personal communication). The formation of the tyrosinate, Y_Z^-, would obviate the need to dissociate the proton prior to the electron transfer and would consequently no longer show a deuterium isotope effect. Tyrosinate formation also represents less of a potential barrier than the formation of the tyrosyl cation radical, as the reduction potential of the latter in solution ($E_{pH<pKa}^0 = 1.5$ V, (*78*)) is far greater than can be generated by the primary electron donor couple, $P680^+$/P680 ($E' = 1.15$ V (*79*)). Finally, site-directed mutants at D1−His190 show a dramatic slowing of Y_Z oxidation (*25*, *43*, *49*, *70*) consistent with a mechanism that requires a handing off of the proton to D1−His190 prior to the electron transfer. These observations together imply that it is the tyrosinate that is the active form in the electron transfer as shown in the upper pathway of Scheme 1. Whether or not the proton transfer is the rate-limiting step in the oxidation of Y_Z will be considered below in two alternative models for coordinated proton and electron transfer.

Model I

Proton-Transfer Limitation. We initially expected to find that the deuterium isotope effect arose from a rate-limiting breakage of the phenolic OH bond. However, transition-state theory (*80*) would argue that the transfer of a proton from Y_Z to D1−His190 in a hydrogen-bonded pair should occur at a rate that approximates 6×10^{12} s^{-1} $\times$ $10^{\Delta pK_a}$ (where ΔpK_a is [$pK_{a[acceptor]} - pK_{a[donor]}$]) or $\sim 6 \times 10^8$ s^{-1}. This rate is substantially faster than the observed rate of oxidation of Y_Z ($\leq 10^6$ s^{-1}) and should not therefore be rate-limiting. On the other hand if Y_Z and D1−His190 are linked indirectly by a hydrogen-bonded chain which might include water molecules, it is possible that a reorganizational process might slow proton transfer sufficiently as to cause such transfer to be rate limiting.

Alternatively, the formation of the hydrogen-bonded Y_Z/D1−His190 pair could be a gated process. The formation of this complex could well involve the breaking of hydrogen bonds formed by Y_Z and D1−His 190 with other partners and the formation of a hydrogen bond with each other in a manner that would be slowed by the replacement of H_2O with D_2O. This is reaction 1 of Scheme 1 and, as in any proton-transfer-limited process, would show the overall rate to be insensitive to the driving force of Y_Z oxidation by $P680^+$. In this model, the deconvolution of the $P680^+$

reduction kinetics would yield fast and slow components with pH-independent rates, arising from centers in the tyrosinate and tyrosine states, respectively, at the time of primary charge separation. As the pH increases, contribution of the faster component should increase and the slower component decrease.

Model II

Electron-Transfer Limitation. It is possible for the Y_Z oxidation rate to be sensitive to the replacement of H_2O with D_2O and yet still be rate-limited by electron transfer. In the upper pathway of Scheme 1, an equilibrium governs the deprotonation of Y_Z (reaction 2). Were the equilibration rapid with respect to Y_Z oxidation and were the tyrosinate the active species for electron transfer, then the rate at a particular pL would be the product of the concentration of tyrosinate and of the intrinsic electron-transfer rate for tyrosinate oxidation. The replacement of H_2O with D_2O in raising the pK_a of tyrosine would lower the tyrosinate concentration through a deuterium isotope effect on the equilibrium. The plot of the deuterium isotope effect in Figure 4B is fit well by the double ratio of $(10^{pL-pK_a}/(1 + 10^{pL-pK_a}))_{H_2O}/(10^{pL-pK_a}/(1 + 10^{pL-pK_a}))_{D_2O}$, which represents such a process and where the pK_a in H_2O is 8.00 and that in D_2O is 8.55. The difference of 0.55 in the pK_a is in good agreement with what has been generally observed for the effect of D_2O on the dissociation of weak acids (*81*). These values for the pK_a are only slightly lower than those estimated for the rate of reduction of $P680^+$ by 0.3 and 0.2 pH units in H_2O and D_2O, respectively. If the tyrosinate/tyrosine equilibration were fast and electron-transfer rate-limiting, then deconvolution of the rate of $P680^+$ reduction would be expected to show a major exponential component, the rate of which should increase with pL. This rate would also be expected to be sensitive to the driving force of the reaction, the difference in the reduction potentials of the redox couples $Y_Z^{\bullet}/Y_Z$ and $P680^+/P680$. An independent study performed at pH 5.7 (unpublished collaboration with Peter Nixon) in which we varied the driving force by site-directed mutagenesis at D1−His198 showed only a weak dependence of the rate of $P680^+$ reduction on the driving force. For example, a mutation (D1−His198Ala) that lowers the potential $P680^+/P680$ by 84 mV relative to wild type slows the electron-transfer rate by only 30%. While such behavior might be expected close to the inverted region of the Marcus curve (*82*), it would imply an unusually low reorganizational energy equivalent to only 90−160 meV (Table 2). A low reorganizational energy seems inconsistent with the disorder that we observe at the Y_Z site.

The pL dependence of the kinetic components that contribute to the $P680^+$ relaxation should provide some guidance in distinguishing between the proton and electron-transfer-limited models discussed above. The actual results of the kinetic deconvolution, however, are complex and appear to depend on the pL. The data in the presence of H_2O appear to support the existence of a pH-dependent rate for the major kinetic component in a biexponential fit. Between pL 5.5 and 7.0 in the presence of D_2O, however, the kinetics are multiphasic (Figure 4A) and are less well-fit by a double exponential, implying the presence of subcomponents that are differentially affected by H/D exchange. This finding is difficult to reconcile with a reaction that is purely electron-transfer-limited. At pL ≥ 7.5, however, both the H_2O and the D_2O data can be well-fit with a biexponential decay with the major component accelerating with increasing pH. The observations presented here are consistent with an increasingly electron-transfer-limited process at pL ≥ 7.5 and a proton-limited process at pL ≤ 7.5. In the upper range of pL, the electron-transfer limitation would likely come from the increased concentration of tyrosinate and possibly also from an acceleration of the Y_Z^-/Y_Z equilibration rate (reaction 2, Scheme 1) or of the gating process (reaction 1, Scheme 1).

Ahlbrink et al. (*77*) have measured the reduction of $P680^+$ with submicrosecond time resolution over a wide range of pH (4−10.5) and fit their data with three exponential components plus an offset. The most rapid ($k_f = 7 \times 10^5$ s^{-1}) and next most rapid ($k_s = 2-10 \times 10^4$ s^{-1}) of these components show only a weak pH dependence (factors of 2 and 5, respectively). The two components also show different kinetic isotope effects (1.6 and 4.0, respectively). These authors propose two equally likely models in which, at high pL, Y_Z oxidation is limited by electron transfer and at low pL by proton transfer. The pK_a (7.0) that separates these two domains is attributed either to that of a proton-accepting base in their Scheme 1A or to Y_Z itself in their Scheme 1B.

We measure here not only a p*K*a for the rate of oxidation of Y_Z but also that for the deuterium isotope effect of the oxidation. We also measure a double difference spectrum for $Y_Z^{\bullet} - Y_Z$ that puts limits on the pK_a of Y_Z^-/Y_Z. The optical and preliminary FTIR data place the pK_a for the deprotonation at between pH 8 and 9. These results all point to the deprotonation of Y_Z as being responsible for the pK_a of 8.0−8.3. While we differ with Ahlbrink et al. (*77*) by 1.0−1.3 in the assignment of the pK_a, the deprotonation of Y_Z corresponds to the second of the two kinetic models they proposed for Mn-depleted PSII core complexes. We prefer a model in which the pK_a of the proton acceptor or of a proton acceptor network is far lower (p*K*a < 5.5) and responsible for the progressive enhancement of charge recombination between Q_A^- and $P680^+$ as the pL is lowered (Figure 9, see also ref *77*).

The proton-limited case and particularly the gated mechanism at pL ≤ 7.5 can explain a number of independent observations in Mn-depleted PSII core complexes. These include the weak dependence of Y_Z oxidation on the driving force of the reaction measured at pH 5.7 (see above) and the mobility of positioning of $Y_Z^{\bullet}$ as judged by ENDOR measurements (*12*, *13*). It also provides an explanation for why, in the intact system, Y_Z oxidation is 100-fold more rapid than in the Mn-depleted case (*85*, *86*) and there is virtually no deuterium isotope effect (*87*−*89*). Ahlbrink et al. (*77*) have attributed these latter observations to a lowering of the pK_a of either the proton acceptor or of Y_Z to 4.5 in the intact system. However, the observations of Noguchi et al. (*22*) and Berthomieu et al. (*25*), using FTIR, of a δC−O−H bending mode for Y_Z at pH 6.0 in the presence of the Mn cluster would appear to be inconsistent with a pK_a of 4.5 for Y_Z. More likely, in light of the above, is a situation in which Y_Z and D1−His190 are locked into a proton-transfer competent complex in the presence of the Mn cluster, no longer as free to move as in its absence. Once this happens, then the proton transfer becomes much faster and the reaction becomes electron-transfer-limited (model II, here and as in Scheme 1A of Ahlbrink et al. (*77*)). The influence of D_2O

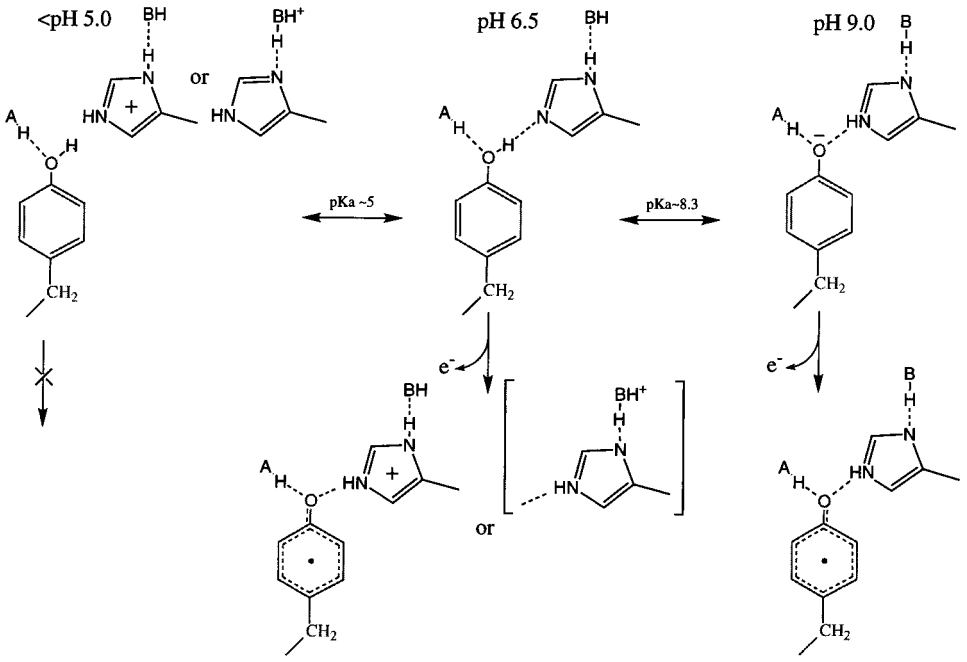

FIGURE 9: Three proposed states of the Y_Z-proton acceptor complex at different pHs. The model assumes D1−His190 as the immediate proton acceptor, though like models could be drawn with other residues or water in between. D1−His190 is also hydrogen bonded to another residue as part of a hydrogen-bonded network. The state at pH < 5.0 is unable to transfer an electron as the proton acceptor is already protonated. The state at pH 6.5 gives the maximum kinetic isotope effect, consistent with the need to form the hydrogen-bonded electron/proton-transfer competent complex as shown for Y_Z oxidation. The state at pH 9.0 shows Y_Z in the tyrosinate state but hydrogen bonded by the proton acceptor. Y_Z oxidation in this state should be electron-transfer-limited with no kinetic isotope effect.

on the equilibrium of reaction 2 (our Scheme 1) would also have to be substantially smaller in this case (less than the 0.55 ΔpK_a observed in the Mn-depleted PSII cores, Figure 4B).

We have been looking, using pulsed ENDOR, for evidence of hyperfine coupling between D1−His190 and $Y_Z^{\bullet}$. We see (Campbell, Britt, and Diner, manuscript in preparation) no sets of ^{15}N ENDOR peaks comparable to the 0.8 MHz hyperfine-coupled feature arising from the imidazole nitrogen of the $Y_D^{\bullet}$/D2−His189 hydrogen-bonded pair (*69*). This observation could be a consequence of a dynamic gating process in which the electron/proton-transfer competent hydrogen-bonded state either is present at low concentration as at room temperature or is frozen out at the low temperature (11 K) of the ENDOR experiment. One prediction of the gated model is that such ^{15}N coupling to $Y_Z^{\bullet}$ should be weak in the absence of the Mn cluster and stronger in its presence. This prediction is currently under investigation.

The pL dependence of the rate for Y_Z oxidation has, as mentioned above, been investigated by Ahlbrink et al. (*77*) in work carried out in parallel and by Lydakis-Simantiris, N., Babcock, G. T., and Golbeck, J. (unpublished results). Possible reasons why Ahlbrink et al. (*77*) find a pK_a 1−1.3 units lower include the source of the PSII core complexes, the manner of their preparation, and the presence of Y_D in Ahlbrink et al. and its absence here. Preliminary experiments of ours also suggest a role for Ca^{2+} in this difference, the present experiments having been performed in the absence of this dication.

The kinetic isotope effect reported here reaches a maximum at pL 7.0 and then decreases as the pL is lowered. This decrease with decreasing pL is likely a reflection of the decreasing equilibrium constant, K_{zp}, and an increasing contribution of $P680^+Q_A^-$ recombination to the kinetics of $P680^+$ reduction (see also ref *77*). As shown earlier (Figure 2), such charge recombination shows no deuterium isotope effect. A possible reason for the lowering of the equilibrium constant as the pH is lowered is the protonation of the proton acceptor itself or of another base to which it is hydrogen bonded in a hydrogen-bonded chain, thereby blocking the deprotonation of Y_Z that would normally accompany oxidation (Figure 9). For example, protonation of histidine imidazole to form the imidazolium ion of D1−His190 would produce a situation similar to that observed upon site-directed replacement of this same residue (*43*, *49*, *70*). Both the mutagenesis and the lowered pH (*77*) slow the oxidation of Y_Z by 3 orders of magnitude.

The pK_a of tyrosine is normally located around 10 in many proteins and possibly higher in a medium of low dielectric. The downshifting of the pK_a for Y_Z^-/Y_Z implies that the pairing of Y_Z with a proton acceptor causes a shift to 8.0−8.3 of the apparent pK_a of tyrosine Y_Z. A more extreme form of this proposal has been put forward by Candeias et al. (*83*) in which both tyrosines Y_Z and Y_D are in the tyrosinate state in all of the UV difference spectra reported in the literature, including those at pH as low as 5.0 (*7*). While we agree that Y_Z is deprotonated at more alkaline pH (pK_a 8.0−8.3), the presence of tyrosinate at pH 5.0 would be inconsistent with the observation of a kinetic isotope effect for Y_Z oxidation, the decrease of this effect with increasing pL, the double difference spectrum of $Y_Z^{\bullet} - Y_Z$ at pH 9.0 minus 6.1 (indicating an increase in tyrosinate concentration as the pL rises), and the presence of a δC−O−H bending mode in the FTIR spectrum of $Y_Z^{\bullet}/Y_Z$ at pH 6.0 (*25*).

Measurements of Q_A^--donor side charge recombination in the presence of H_2O and D_2O indicate an acceleration of charge recombination by the latter, more marked at lower than at higher pL (Table 2). This observation implies a

lowering of the K_{zp} equilibrium constant by D_2O at pL $\leq$ 8.0. The rate of reduction of $Y_Z^\bullet$ by P680 (k_b) shows only a slight dependence on pL, in basic agreement with the observations of Yerkes et al. (*85*), indicating that the pH dependence of K_{zp} comes largely from k_f. The rate constant, k_b, changes by no more than a factor of 2 over the same pL range (5.5−9.5) that gives a rate increase of a factor of 40 and 100 for H_2O and D_2O, respectively. There exists a deuterium isotope effect of only about 2 for k_b, and the ratio $k_b(H)/k_b(D)$ is insensitive to pL over the range studied. This small kinetic isotope effect is probably associated with solvent reorganization that accompanies $Y_Z^\bullet$ reduction. The source of the proton involved in the reduction of Y_Z is likely to remain the same over this pL range and is most likely one of the two in hydrogen-bonded contact with the phenolic oxygen of the radical. These observations imply that the reduction of $Y_Z^\bullet$ is not limited by proton transfer and it is likely that the electron transfer precedes the proton transfer.

A number of authors (*84*, *87*, *88*, *90*) have recently measured kinetic deuterium isotope effects for the advance of each of the S-states of the Mn cluster coupled to the reduction of Y_Z. With the exception of S2 → S3 for which values of up to 2.4 have been reported, the other S-state transitions show kinetic deuterium isotope effects of 1.6 or less. It has been suggested that only in the S2 → S3 transition is there proton-coupled electron transfer (*35*). As pointed out above, the likelihood of electron transfer preceding proton transfer for the reduction of $Y_Z^\bullet$ and the observation of a kinetic isotope effect of about 2 in the absence of the Mn cluster are likely to limit the utility of the observed kinetic deuterium isotope effects to conclude whether hydrogen atom (or electron plus proton) abstraction by Y_Z has occurred on the S-state transitions, except where the energetics require that the electron and the proton move together. This may be the case for S2 → S3. Indeed, the driving force for the oxidation of S2 by $Y_Z^\bullet$ has been estimated to be quite small (*91*), possibly requiring the added boost that comes from the difference in OH bond energies between tyrosine and water bound to Mn. While there is some risk in extrapolating from kinetic measurements of Y_Z reduction in the absence of the Mn cluster to those in its presence, FTIR difference spectra for Y_Z oxidation appear to be virtually the same in the two cases (*25*).

Communication with Solvent. Upon injection into D_2O, the more rapid replacement of the phenolic OH with OD for $Y_Z^\bullet$ as compared to $Y_D^\bullet$ indicates that Y_Z is in far more rapid communication with the solvent. This observation is shared by Lydakis-Simantiris, N., Babcock, G. T., and Golbeck, J. (unpublished results) and by refs *52* and *77*. The greater accessibility of water to Y_Z may also explain why the reduction potential of $Y_Z^\bullet/Y_Z$ is actually closer to that of tyrosine in aqueous solution than in the case of $Y_D^\bullet/Y_D$. This greater accessibility is consistent with a closer proximity of Y_Z to exogenous electron donors, including Mn^{2+}, and to the Mn cluster, itself accessible to solvent water. The principal argument for close proximity of $Y_Z^\bullet$ and the Mn cluster is the demonstration that the split signal arises from the coupling between an organic radical (*92*), now known to be a tyrosyl radical, most likely $Y_Z^\bullet$ (*14*, *26*, *29*, *35*, *73*), and the Mn cluster.

The rapid communication between Y_Z and bulk solvent in the absence of the Mn cluster may not be an entirely accurate reflection of the environment of the tyrosine in the presence of the cluster. In fact an enhanced accessibility to water upon extraction of the cluster could increase the reorganizational energy associated with Y_Z oxidation and explain in part the slowing of the rate of Y_Z oxidation by close to 2 orders of magnitude following removal of the cluster (*85*, *86*). Force et al. (*57*) and Tommos et al. (*52*) have found that, in the presence of the Mn cluster, H/D exchange of hydrogen bonds associated with the S2−$Y_Z^\bullet$ split signal is rapid ($t_{1/2}$ < 40 min). However, as indicated below, such exchange may be occurring at the cluster itself rather than at the level of Y_Z. These data may therefore still be consistent with an enhanced access of Y_Z to solvent upon removal of the Mn cluster. As pointed out above, other explanations for the more rapid electron transfer in the intact system involve locking Y_Z and the proton acceptor into a proton-transfer competent complex that makes the proton transfer much faster than the electron transfer. If there were reduced accessibility of solvent water to the site, then the reduced effect of H_2O/D_2O exchange on the pK_a of Y_Z in the intact system (see above) also becomes more understandable. These kinetic and potentially structural differences exist despite indications from FTIR that the protein vibrational modes coupled to the oxidation of Y_Z are largely independent of the presence or absence of the Mn cluster (*25*).

Numbers of Hydrogen Bonds. An ESEEM comparison, using ENDOR-derived coupling constants, shows that the numbers of $^1H/^2H$ exchangeable hydrogen-bonded protons in contact with $Y_D^\bullet$ are two and one, respectively, in Mn-depleted *Synechocystis* PSII core complexes and in BBY PSII-enriched membranes. While the ENDOR for $Y_Z^\bullet$ does not provide well-defined coupling constants, the ESEEM spectrum of this radical can be well-simulated by two hydrogen bonds using the coupling constants described in the Results. However, given the clear disorder in the hyperfine couplings, reflected in the poorly resolved ^2H ENDOR spectrum (*13*), there appears to be a distribution in hydrogen bonding to $Y_Z^\bullet$ in the Mn-depleted *Synechocystis* core complexes. Some centers may indeed have two hydrogen bonds, while some fraction may have only one with additional proximal deuterons adding to the modulation.

This observation for *Synechocystis* $Y_D^\bullet$ is in contrast with the apparent complete loss of a hydrogen-bonded proton in the ENDOR spectrum of mutant D2−His189Gln (*47*). While it is possible that the structural change associated with this mutation results in the coincident loss of two hydrogen bonds, high field EPR of the mutant shows a value of g_x (2.00832) larger than that of wild type (2.00740) but also smaller than that of *E. coli* ribonucleotide reductase (2.00868). The g_x component of the anisotropic g tensor for the tyrosyl radical is an indicator of hydrogen bonding. While there may be other electrostatic factors that contribute to g_x, the value for g_x could imply that for the mutant there is greater hydrogen bonding to the phenolic oxygen than in the case of *E. coli* ribonucleotide reductase tyrosyl radical Y122$^\bullet$ which is thought to be hydrogen-bond-free. The hydrogen-bonding characteristics of the D2−His189Gln mutant are currently undergoing further examination.

The situation for the S2−$Y_Z^\bullet$ split signal in Ca^{2+}-depleted and in acetate-treated BBYs, originally thought to reflect two hydrogen bonds to $Y_Z^\bullet$ (*52*, *57*), is now understood to be more complicated by the combined exchange and dipolar

coupling (*29*, *73*) between S2 and $Y_Z^\bullet$. As a result, the ESEEM spectrum may show contributions from H/D exchange at the Mn cluster as well as at $Y_Z^\bullet$ such that the fit to two exchangeable hydrogen bonds may be fortuitous.

The similarity in the number of hydrogen bonds to $Y_Z^\bullet$ and $Y_D^\bullet$ in *Synechocystis* is consistent with another indicator of hydrogen bonding, the g_x component of the anisotropic *g* tensor, 2.0075 and 2.0074, respectively (*74*). However, an apparent heterogeneity in the hydrogen bonding of $Y_Z^\bullet$ as revealed in the greater breadth of the high field EPR g_x component (*74*) and in the deuterium coupling for $Y_Z^\bullet$ in pulsed ^{2}H ENDOR (*13*) as compared to $Y_D^\bullet$ suggests that the two hydrogen bonds are more equivalent in the case of $Y_D^\bullet$ than they are for $Y_Z^\bullet$. This difference in hydrogen bonding is also revealed in the FTIR spectra of the two tyrosyl radicals where $Y_Z^\bullet$ would appear to be more interactive in hydrogen bonding than $Y_D^\bullet$ or where, alternatively, there is a greater retention of positive charge in the environment of $Y_D^\bullet$ than $Y_Z^\bullet$ (*21*, *25*). What consequence these differences have for the 250−300 mV difference in reduction potential between these two tyrosines is still unclear.

It has been proposed that $Y_Z^\bullet$ can act as a hydrogen atom (*36*, *37*) or a proton abstractor (*14*) from water bound to the Mn cluster. Were $Y_Z^\bullet$ hydrogen bonded by two protons in the presence (*52*, *57*, but see qualification above) or absence of the Mn cluster (this work), then proton transfer to $Y_Z^\bullet$ upon its reduction could occur from either source unless some mechanism existed to discriminate between the two. Furthermore, it is likely that the proton that leaves Y_Z upon its oxidation is retained in a hydrogen bond and not immediately released into the thylakoid lumen (*10*, *77*, *93*, but see *52*). Such retention does not exclude a proton being released into the lumen that is either liberated at the other end of a hydrogen-bonded chain or as a Bohr proton. The existence of a Y_Z-proton-acceptor hydrogen-bonded structure implies that, even if one of the hydrogen bonds were to come from water bound to the Mn cluster, there would have to be a selective mechanism, whether kinetic or thermodynamic, to allow for $Y_Z^\bullet$ to choose for proton abstraction, only that proton bound to water and not the one bound to the proton acceptor. A lowering, upon Mn oxidation, of the pK_a of a water bound to Mn could provide such selectivity. It would then be necessary for the proton acceptor that becomes protonated when Y_Z is oxidized to release its proton to a sink other than Y_Z itself. The proposed lumenal release (*36*) of the proton originating from tyrosine would have to occur following $Y_Z^\bullet$ reduction and not coincident with its oxidation.

ACKNOWLEDGMENT

The authors are grateful to Mary Jane Reeve for her excellent technical assistance in the isolation of Photosystem II core complexes and to Dexter Chisholm for his engineering of the *Synechocystis* D2−Tyr160Phe mutant. The authors are also grateful to Drs. Gerald Babcock, Catherine Berthomieu, Richard Debus, Michael Haumann, Jérôme Lavergne, Melvin Okamura, Mark Paddock, and Fabrice Rappaport for their constructive criticism and helpful discussion.

REFERENCES

1. Diner, B. A., and Babcock, G. T. (1996) in *Oxygenic Photosynthesis: The Light Reactions* (Ort, D. R., and Yocum, C. F., Eds.) pp 213−247, Kluwer Academic Publishers, Dordrecht, The Netherlands.
2. Debus, R. J., Barry, B. A., Babcock, G. T., and McIntosh, L. (1988) *Proc. Natl. Acad. Sci. U.S.A. 85*, 427−430.
3. Debus, R. J., Barry, B. A., Sithole, I., Babcock, G. T., and McIntosh, L. (1988) *Biochemistry 27*, 9071−9074.
4. Vermaas, W. F. J., Rutherford, A. W., and Hansson, Ö. (1988) *Proc. Natl. Acad. Sci. U.S.A. 85*, 8477−8481.
5. Metz, J. G., Nixon, P. J., Rögner, M., Brudvig, G. W., and Diner, B. A., (1989) *Biochemistry 28*, 6960−6969.
6. Koulougliotis, D., Tang, X.-S., Diner, B. A., and Brudvig, G. W. (1995) *Biochemistry 34*, 2850−2856.
7. Dekker, J. P., van Gorkom, H. J., Brok, M., and Ouwehand, L. (1984) *Biochim. Biophys. Acta 764*, 301−309.
8. Diner, B. A., and de Vitry, C. (1984) in *Advances in Photosynthesis Research* (Sybesma, C., Ed.) Vol 1, pp 407−411, Martinus Nijhoff/Dr. W. Junk, The Hague, The Netherlands.
9. Renger, G., and Weiss, W. (1986) *Biochim. Biophys. Acta 850*, 184−196.
10. Diner, B. A., Tang, X.-S., Zheng, M., Dismukes, G. C., Force, D. A., Randall, D. W., and Britt, R. D. (1995) in *Photosynthesis: from Light to Biosphere* (Mathis, P., Ed.) Vol 2, pp 229−234, Kluwer Academic Publishers, Dordrecht, The Netherlands.
11. Barry, B. A., and Babcock, G. T. (1987) *Proc. Natl. Acad. Sci. U.S.A. 84*, 7099−7103.
12. Tommos, C., Tang, X.-S., Warncke, K., Hoganson, C. W., Styring, S., McCracken, J., Diner, B. A., and Babcock, G. T. (1995) *J. Am. Chem. Soc. 117*, 10325−10335.
13. Force, D. A., Randall, D. W., Britt, R. D., Tang, X.-S., and Diner, B. A. (1995) *J. Am. Chem. Soc. 117*, 12643−12644.
14. Gilchrist, M. L., Ball, J. A., Randall, D. W., and Britt, R. D. (1995) *Proc. Natl. Acad. Sci. U.S.A. 92*, 9545−9549.
15. Tang, X.-S., Zheng, M., Chisholm, D. A., Dismukes, G. C., and Diner, B. A. (1996) *Biochemistry 35*, 1475−1484.
16. Hoganson, C. W., and Babcock, G. T. (1992) *Biochemistry 31*, 11874−11880.
17. Rigby, S. E. J., Nugent, J. H. A., and O'Malley, P. J. (1994) *Biochemistry 33*, 1734−1742.
18. Evelo, R. G., Hoff, A. J., Dikanov, S. A., and Tyryshkin, A. M. (1989) *Chem. Phys. Lett. 161*, 479−484.
19. Warncke, K., McCracken, J., and Babcock G. T. (1994) *J. Am. Chem. Soc. 116*, 7332−7340.
20. Hienerwadel, R., Boussac, A., Breton, J., and Berthomieu, C. (1996) *Biochemistry 35*, 15447−15460.
21. Hienerwadel, R., Boussac, A., Breton, J., Diner, B. A., and Berthomieu, C. (1997) *Biochemistry 36*, 14712−14723.
22. Noguchi, T., Inoue, Y., and Tang, X.-S. (1997) *Biochemistry 36*, 14705−14711.
23. MacDonald, G. M., Bixby, K. A., and Barry, B. A. (1993) *Proc. Natl. Acad. Sci. U.S.A. 90*, 11024−11028.
24. Zhang, H., Razeghifard, M. R., Fischer, G., and Wydrzynski, T. (1997) *Biochemistry 36*, 11762−11768.
25. Berthomieu, C., Hienerwadel, R., Boussac, A., Breton, J., and Diner, B. A. (1998) *Biochemistry 37*, 10547−10554.
26. Tang, X.-S., Randall, D. W., Force, D. A., Diner, B. A., and Britt, R. D. (1996) *J. Am. Chem. Soc. 118*, 7638−7639.
27. Hallahan, B. J., Nugent, J. H. A., Warden, J. T., and Evans, M. C. W. (1992) *Biochemistry 31*, 4562−4573.
28. Deak, Z., Vass, I., and Styring, S. (1994) *Biochim. Biophys. Acta 1185*, 65−74.
29. Peloquin, J. M., Campbell, K. A., and Britt, R. D. (1998) *J. Am. Chem. Soc. 120*, 6840−6841.
30. Lind, J., Shen, X., Eriksen, T. E., and Merényi, G. (1990) *J. Am. Chem. Soc. 112*, 479−482.
31. Krishtalik, L. I. (1990) *Bioelectrochem. Bioenerg. 23*, 249−263.
32. Haumann, M., and Junge, W. (1994) *Biochemistry 33*, 864−872.
33. Gardner, K. A., and Mayer, J. M. (1995) *Science 269*, 1849−1851.
34. Baldwin, M. J., and Pecoraro, V. L. (1996) *J. Am. Chem. Soc. 118*, 11325−11326.

35. Szalai, V. A., and Brudvig, G. W. (1996) *Biochemistry 35*, 15080−15087.
36. Hoganson, C. W., Lydakis-Simantiris, N., Tang, X.-S., Tommos, C., Warncke, K., Babcock, G. T., Diner, B. A., McCracken, J., and Styring, S. (1995) *Photosynth. Res. 46*, 177−184.
37. Babcock, G. T., Espe, M., Hoganson, C., Lydakis-Simantiris, N., McCracken, J., Shi, W., Styring, S., Tommos, C., and Warncke, K. (1997) *Acta Chem. Scand. 51*, 533−540.
38. Paddock, M. L., Rongey, S. H., McPherson, P. H., Juth, A., Feher, G., and Okamura, M. Y. (1994) *Biochemistry 33*, 734−745.
39. Ruffle, S. V., Donnelly, D., Blundell, T. L., and Nugent, J. H. A. (1992) *Photosynth. Res. 34*, 287−300.
40. Svensson, B., Vass, I., Cedergren, E., and Styring, S. (1990) *EMBO J. 9*, 2051−2059.
41. Svensson, B., Etchebest, C., Tuffery, P., van Kan, P., Smith, J., and Styring, S. (1996) *Biochemistry 35*, 14486−14502.
42. Babcock, G. T., and Sauer, K. (1975) *Biochim. Biophys. Acta 396*, 48−62.
43. Diner, B. A., Nixon, P. J., and Farchaus, J. W. (1991) *Curr. Opin. Struct. Biol. 1*, 546−554.
44. Roffey, R., van Wijk, K., Sayre, R., and Styring, S. (1994) *J. Biol. Chem. 269*, 5115−5121.
45. Tommos, C., Davidsson, L., Svensson, B., Madsen, C., Vermaas, W., and Styring, S. (1993) *Biochemistry 32*, 5436−5441.
46. Tommos, C., Madsen, C., Styring, S., and Vermaas, W. (1994) *Biochemistry 33*, 11805−11813.
47. Tang, X.-S., Chisholm, D. A., Dismukes, G. C., Brudvig, G. W., and Diner, B. A. (1993) *Biochemistry 32*, 13742−13748.
48. Chu, H.-A., Nguyen, A. P., and Debus, R. J. (1995) *Biochemistry 34*, 5839−5858.
49. Hays, A.-M. A., Vassiliev, I. R., Golbeck, J. H., and Debus, R. J. (1998) *Biochemistry 37*, 11352−11365.
50. Innes, J. B., and Brudvig, G. W. (1989) *Biochemistry 28*, 1116−1125.
51. Isogai, Y., Itoh, S., and Nishimura, M. (1990) *Biochim. Biophys. Acta 1017*, 204−208.
52. Tommos, C., McCracken, J., Styring, S., and Babcock, G. T. (1998) *J. Am. Chem. Soc. 120*, 10441−10432.
53. Williams, J. G. K. (1988) *Methods Enzymol. 167*, 766−778.
54. Berthold, D. A., Babcock, G. T., and Yocum, C. F. (1981) *FEBS Lett. 134*, 231−234.
55. Ford, R. C., and Evans, M. C. W. (1983) *FEBS Lett. 160*, 159−164.
56. Kim, D. H., Britt, R. D., Klein, M. P., and Sauer, K. (1992) *Biochemistry 31*, 541−547.
57. Force, D. A., Randall, D. W., and Britt, R. D. (1997) *Biochemistry 36*, 12062−12070.
58. MacLachlan, D. J., and Nugent, J. H. A. (1993) *Biochemistry 32*, 9772−9780.
59. Joliot, P., Béal, D., and Frilley, B. J. (1980) *Chim. Phys. 77*, 209−216.
60. Sturgeon, B. E., and Britt, R. D. (1992) *Rev. Sci. Instrum. 63*, 2187−2192.
61. Mims, W. B., and Peisach, J. (1981) in *Biological Magnetic Resonance* (Berliner, L. J., and Ruben, J., Eds.) pp 213−263, Plenum Press, New York.
62. Britt, R. D. (1996) *in Biophysical Techniques in Photosynthesis* (Amesz, J., and Hoff, A. J., Eds.) pp 137−164, Kluwer Academic, Dordrecht, The Netherlands.
63. Mims, W. B. (1984) *J. Magn. Reson. 59*, 291−306.
64. Britt, R. D., Zimmermann, J.-L., Sauer, K., and Klein, M. P. (1989) *J. Am. Chem. Soc. 111*, 3522−3532.
65. Mims, W. B. (1972) in *Electron Paramagnetic Resonance* (Geschwind, S., Ed.) pp 263−351, Plenum Press, New York.
66. Buser, C. A., Diner, B. A., and Brudvig, G. W. (1990) *Biochemistry 29*, 8977−8985.
67. Un, S., Tang, X.-S., and Diner, B. A. (1996) *Biochemistry 35*, 679−684.
68. Rodriguez, I. D., Chandrashekar, T. K., and Babcock, G. T. (1987) in *Progress in Photosynthesis* (Biggins, J., Ed.) Vol 1, pp 471−474, Martinus Nijhoff Publishers, Dordrecht, The Netherlands.
69. Campbell, K. A., Peloquin, J. M., Diner, B. A., Tang, X.-S., Chisholm, D. A., and Britt, R. D. (1997) *J. Am. Chem. Soc. 119*, 4787−4788.
70. Diner, B. A., and Nixon, P. J. (1998) in *Proceedings of the Eleventh International Congress on Photosynthesis* (Garab, G., Ed.) Kluwer Academic Publishers, Dordrecht, The Netherlands.
71. Conjeaud, H., and Mathis, P. (1980) *Biochim. Biophys. Acta 590*, 353−359.
72. Buser, C. A., Diner, B. A., and Brudvig, G. W. (1990) *Biochemistry 29*, 8977−8985.
73. Dorlet, P., Di Valentin, V., Babcock, G. T., and McCracken, J. L. (1998) *J. Phys. Chem*. (submitted for publication).
74. Un, S., Tang, X.-S., and Diner, B. A. (1996) *Biochemistry 35*, 679−684.
75. Conjeaud, H., and Mathis, P. (1980) *Biochim. Biophys. Acta 590*, 353−359.
76. Reinman, S., Mathis, P., Conjeaud, H., and Stewart, A. (1981) *Biochim. Biophys. Acta 635*, 429−433.
77. Ahlbrink, R., Haumann, M., Cherapanov, D., Bögenshausen, O., Mulkidjanian, A., and Junge, W. (1998) *Biochemistry 37*, 1131−1142.
78. Harriman, A. (1987) *J. Phys. Chem. 91*, 6102−6104.
79. Klimov, V. V., and Krasnovskii, A. A. (1981) *Photosynthetica 15*, 592−609.
80. Fersht, A. (1985) *Enzyme Structure and Mechanism*, p 48, W. H. Freeman and Co., New York.
81. Quinn, D. M., and Sutton, L. D. (1991) in *Enzyme Mechanism from Isotope Effects* (Cook, P. F., Ed.) p 107, CRC Press, Boca Raton, FL.
82. Marcus, R. A., and Sutin, N. (1985) *Biochim. Biophys. Acta 811*, 265−322.
83. Candeias, L. P., Turconi, S., and Nugent, J. H. A. (1998) *Biochim. Biophys. Acta 1363*, 1−5.
84. Karge, M., Irrgang, K.-D., Sellin, S., Feinäugle, R., Liu, B., Eckert, H.-J., Eichler, H. J., and Renger, G. (1996) *FEBS Lett. 378*, 140−144.
85. Yerkes, C. T., Babcock, G. T., and Crofts, A. R. (1983) *FEBS Lett. 158*, 359−363.
86. Brettel, K., Schlodder, E., and Witt, H. T. (1984) *Biochim. Biophys. Acta 766*, 403−415.
87. Karge, M., Irrgang, K.-D., and Renger, G. (1997) *Biochemistry 36*, 8904−8913.
88. Haumann, M., Bögershausen, O., Cherepanov, D., Ahlbrink, R., and Junge, W. (1997) *Photosynth. Res. 51*, 193−208.
89. Schilstra, M. J., Rappaport, F., Nugent, J. H. A., Barnett, C. J., and Klug, D. R. (1998) *Biochemistry 37*, 3974−3981.
90. Lydakis-Simantiris, N., Ghanotakis, D. F., and Babcock, G. T. (1997) *Biochim. Biophys. Acta 1322*, 129−140.
91. Shinkarev, V. P., and Wraight, C. (1993) *Proc. Natl. Acad. Sci. U.S.A. 90*, 1834−1838.
92. Boussac, A., Zimmermann, J.-L., Rutherford, A. W., and Lavergne, J. (1990) *Nature 347*, 303−306.
93. Rappaport, F., and Lavergne, J. (1997) *Biochemistry 36*, 15294−15302.

BI981894R